HHS Public Access

Author manuscript

Nat Neurosci. Author manuscript; available in PMC 2010 August 01.

Published in final edited form as:

Nat Neurosci. 2010 February ; 13(2): 239–245. doi:10.1038/nn.2475.

A neural mechanism for exacerbation of headache by light

Rodrigo Noseda[1], **Vanessa Kainz**[1], **Moshe Jakubowski**[1], **Joshua J. Gooley**[2], **Clifford B. Saper**[2,3], **Kathleen Digre**[4], and **Rami Burstein**[1,3]

[1]Department of Anesthesia, Harvard Medical School, Boston, Massachusetts, USA

[2]Department of Neurology, Harvard Medical School, Boston, Massachusetts, USA

[3]Beth Israel Deaconess Medical Center and Program in Neuroscience, Harvard Medical School, Boston, Massachusetts, USA

[4]Department of Neurology and Ophthalmology, Moran Eye Center, University of Utah, Salt Lake City, Utah

Abstract

The perception of migraine headache, which is mediated by nociceptive signals transmitted from the cranial dura mater to the brain, is uniquely exacerbated by exposure to light. Here we show that exacerbation of migraine headache by light is prevalent among blind persons who maintain non-image-forming photoregulation in the face of massive rod/cone degeneration. Using single-unit recording and neural tract-tracing in the rat, we identified dura-sensitive neurons in the posterior thalamus, whose activity was distinctly modulated by light, and whose axons projected extensively across layers I through V of somatosensory, visual and associative cortices. The cell bodies and dendrites of such dura/light-sensitive neurons were apposed by axons originating from retinal ganglion cells, predominantly from intrinsically-photosensitive retinal ganglion cells – the principle conduit of non-image-forming photoregulation. We propose that photoregulation of migraine headache is exerted by a non-image-forming retinal pathway that modulates the activity of dura-sensitive thalamocortical neurons.

Migraine is a recurring, episodic neurological disorder characterized as a unilateral, throbbing headache that is commonly associated with a variety of other symptoms (e.g., nausea, vomiting, irritability, fatigue)[1],[2]. Migraine pain is thought to originate from chemical irritation of the meninges, which leads to transmission of nociceptive signals from the dura mater to the brain via the so-called trigeminovascular pathway[3]. The first- and second-order neurons in this pathway are, respectively, sensory neurons in the trigeminal ganglion that project centrally to the spinal trigeminal nucleus (SpV)[4], and dura-sensitive neurons in laminae I and V of SpV that project to the posterior thalamus[5]. Prolonged neuronal activation during a migraine attack is thought to induce peripheral and central

Correspondence – Rami Burstein, CLS-649, 330 Brookline Avenue, Boston, MA 02215, USA; Tel: 617 735-2832, fax: 617 735-2833, rburstei@bidmc.harvard.edu.

Author Contributions: R.B., M.J. and R.N. designed the study. R.N., V.K., J.J.G, and R.B. conducted the various experiments. M.J., R.N., C.B.S., and K.D. contributed to data analysis and presentation. R.B. and M.J. wrote the manuscript.

sensitization along the trigeminovascular pathway, which explains the throbbing of headache[6] and the accompanying scalp and neck-muscle tenderness[7], and whole-body cutaneous allodynia[8].

The perception of migraine headache is uniquely exacerbated during exposure to ambient light as compared to the pain level felt in the dark[9,10]. Other forms of abnormal light sensitivity, commonly referred to as photophobia, are typically associated with anterior segments disorders of the eye such as uvetis, cyclitis, iritis, and blepharitis[11], and intracranial pathologies such as meningitis, subdural hemorrhage, and intracranial tumors[9,12–14]. Unlike forms of photophobia defined as abnormal light sensitivity[11], or ocular discomfort induced by light (also termed photo-oculodynia)[15], we postulated that exacerbation of migraine headache by light[10,16] is driven by photic signals transmitted from the retina via the optic nerve to central neurons that process nociceptive signals from the meninges.

Retinal projections to the brain constitute image-forming and non-image-forming pathways. Image formation in vertebrates – the tracking and interpreting visual objects and patterns – is generated primarily by photoactivation of the classic opsin-based photopigments of retinal rods and cones, and subsequent activation of retinal ganglion cells (RCG), whose axons project to visual cortices via the optic nerve, the lateral geniculate nucleus (LGN), and the superior colliculus. Non-image forming functions in vertebrates, including the entrainment of the biological clock to the dark-light cycle, adaptation of pupillary size to light[17], and suppression of melatonin release by light[18], are all mediated by a specialized pathway originating from intrinsically-photosensitive RGC (ipRGC), whose axons project via the optic nerve to the suprachiasmatic nucleus (SCN), intergeniculate leaflet (IGL) and olivary pretectal nucleus (OPT)[17,19–25]. Activation of ipRGC is achieved not only extrinsically by rods and cones, but also intrinsically by virtue of their unique photopigment known as melanopsin[20,26–30].

The neural mechanism for the photic exacerbation of migraine headache is unknown. Also unknown is whether central trigeminovascular neurons can be modulated, either directly or indirectly, by photic signals from the retina. Here we show that exacerbation of headache by light is preserved in blind migraineurs that rely primarily on non-image-forming photoreception, but absent in those who lost their optic nerve or the eyes. We also show that light modulates the activity of a subset of trigeminovascular thalamic neurons that receive input from the retina and project to multiple cortical areas.

Results

Photophobia in blind migraine patients

The prevalence of migraine-associated photophobia was documented in 20 blind migraine sufferers (15 females, 5 males). Their demographic profile was similar to that of migraineurs with normal eyesight in terms of age (43.5 ± 3.4 years; mean ± s.e.m.); age at the time of first migraine attack (17.8 ± 2.9); years of migraine history (25.8 ± 3.8); frequency of attacks (6.4 ± 1.9 per month); incidence of visual aura (35% of patients).

Six of the patients had no light perception due to bilateral enucleation of the eyes, or damage to the optic nerves (Table 1). Surgical eye removal was done due to retinal detachment caused by retinal prematurity resulting from neonatal overexposure to oxygen (two cases), retinal cancer (one case), or congenital syphilis/secondary glaucoma (one case). Optic nerve lesions were caused by bilateral optic neuropathy (one case) or extensive hemorrhage (one case). As with mice lacking rods, cones, and melanopsin[30], these subjects suffered irregular or fragmented sleep pattern, and exhibited deficient pupillary light response (PLR). The intensity of their headache was unaffected by light, suggesting that migraine photophobia depends on signals relayed from the retina to the brain via the optic nerve.

Fourteen blind individuals were capable of detecting light in the face of markedly deficient image-forming perception (<20/200 vision; <10° visual field). Eight subjects were diagnosed with inherited retinal degeneration (retinitis pigmentosa, Leber's congenital amaurosis, or cone-rod dystrophy); three had retinal detachment due to neonatal overexposure to oxygen (retinopathy of prematurity); the remaining three were diagnosed with bilateral optic neuropathy, bilateral retinal detachment and glaucoma, or shock optic neuropathy after a large hemorrhage (Table 1). Using interviews, medical records, or direct examination, we found these patients to have normal PLR and regular sleep pattern (in three cases, sleep pattern was disrupted and PLR data were unavailable). In this group, migraine headache intensity under ambient light was rated 9.2 ± 0.2 on a 0–10 subjective scale, compared to 6.2 ± 0.3 in a dim or dark environment. The preservation of migraine photophobia in the face of rod/cone degeneration has led us to investigate whether central trigeminovascular neurons can be regulated by non-image-forming signals from the eye.

Anterograde tracing of RGC projections to the thalamus

We previously mapped retinal projections to non-image-forming brain areas in the rat using intravitreal injections of cholera toxin subunit B (CTB) and recombinant adeno-associated virus containing a green fluorescent protein reporter gene (rAAV–GFP)[22]. Using material from those experiments, we searched for retinal axons in brain areas containing dura-sensitive neurons, including the SpV, parabrachial nucleus, posterior thalamic nuclear group, and ventral posteromedial thalamic nucleus (VPM)[31–33]. Among those, only the dorsocaudal region of the posterior thalamic nuclear group (mostly contralateral to the injected eye) contained anterogradely-labeled retinal axons (Fig. 1). Viewed in a parasagittal plane (Supplementary Fig. 1), fibers labeled by intravitreal injection of 1% CTB descended ventrorostrally from the main visual pathway toward the dorsal aspect of the posterior thalamic nuclear group, between the anterior pretectal (APT) and the lateral posterior thalamic nuclei.

Retinal input into posterior thalamic nuclear group was examined in 9 rats that received a large intravitreal injections of rAAV–GFP (1.7×10^{10} viral particles in 10 μl), and in 3 rats that received a smaller amount of the tracer (8.5×10^{9} particles in 5 μl). Axonal labeling in the caudal portion of the posterior thalamus was examined in a series of coronal sections stretching about 1 mm rostro-caudally (−3.7 to −4.5 mm from Bregma; Fig. 1). The larger injection of the tracer produced heavy axonal labeling in the optic tract and the main visual thalamic nuclei, including all subdivisions of the LGN and the brachium superior colliculus

(Fig. 1a). The smaller injection of the tracer, however, yielded heavy axonal labeling primarily in the IGL (Fig. 1b) and OPT, reflecting preferential uptake by ipRGC[22]. Despite these marked differences, both methods of injection yielded similar pattern and density of labeled axons in the ventral part of lateral posterior thalamic nuclei and the dorsal part of posterior thalamic nuclear group (Fig. 1). Individual retinal axons in the dorsal aspect of the posterior thalamic nuclear group are shown at higher power in Supplementary Fig. 2.

Injection of the retrograde tracer Fluorogold into the posterior thalamic nuclear group resulted in simultaneous labeling of cell bodies in laminae I and V of the contralateral SpV, and retinal ganglion cells, including melanopsinergic ipRGC, in the contralateral eye (Supplementary Fig. 3, 4). We therefore set out to search for individual thalamic neurons that process and integrate nociceptive signals from the meninges (mediated by trigeminovascular SpV neurons) and photic signals from the eye.

Effects of light on dura-sensitive thalamic neurons

Using extracellular single-unit recording in deeply anesthetized rats, we identified 20 units in the posterior thalamus that responded to stimulation of the dura (Fig. 2a,b; Supplementary Fig. 5), 14 of which were also photosensitive. Compared with their ongoing activity in the dark, mean firing rate of the 20 dura-sensitive units increased about 2-fold in response to ambient fluorescence light (500 lux), and 4-fold in response to bright light (50,000 lux) shone directly on the contralateral eye (Fig. 2c). For control, we studied 14 units that were unresponsive to stimulation of the dura; those units were found to be unresponsive to ambient light as well (Fig. 2c). Histological analysis of the recording sites indicated that most dura/light-sensitive neurons (9/13) were localized at or above the dorsal border of the posterior thalamic nuclear group (Fig. 2d,e; red label). Dura-sensitive units that were unresponsive to light were found more ventrally in posterior thalamic nuclear group proper, as well as in VPM and the ventral posterolateral thalamic nucleus (Fig. 2d,e; blue label). Control units, which were neither dura-sensitive nor light-sensitive, were present in all of the regions mentioned above (Fig. 2d,e; black label).

Latencies of neuronal photoactivation were measured using 3 levels of illuminance. Illuminance of the contralateral eye with 50,000 lux induced delayed activation in 7 units (3, 4.4, 5, 5, 6, 20, 24 s latencies; Fig. 2f) and rapid activation in another set of 7 units (<1 s; Fig. 2g). Binocular ambient illuminance with 3,000 lux induced delayed activation in 5 units (2, 20, 200, 200, 280 s latencies; Fig. 2h), and rapid activation (<1 s) in 2 units that were tested repeatedly (Fig. 2i); the latter latencies averaged 295 ± 66 ms in one unit (9 trials ranging 48–619 ms) and 426 ± 141 ms in the other (5 trials ranging 243–983 ms). Ambient illuminance with 500 lux (ceiling fixtures of fluorescent light) induced delayed activation in 4 units (170, 190, 210 and 340 s latencies, Fig. 2j) and rapid activation in 3 units (<1 s). Latencies for rapid activation with 50,000 and 500 lux could not be measured at ms resolution, because the light source was not synchronized with the data acquisition software. The wide range of response latencies led us to evaluate the anatomical relationships between retinal afferents and individual dura-sensitive neurons in the posterior thalamus.

Retinal afferents to thalamic dura/light-sensitive units

Retinal afferents were traced anterogradely by injecting 6 μl 1% CTB into the vitreous body of one eye under brief isoflurane anesthesia. Three days later, individual dura/light-sensitive neurons (one neuron/rat) were identified in the contralateral posterior thalamus using a recording glass micropipette (20 mˆ) under extended isoflurane anesthesia. A neuron thus identified was then filled with the anterograde tracer tetramethylrhodamine–dextran conjugate (TMR–dextran) which was preloaded into the recording micropipette. Juxtacellular iontophoresis of the tracer into the target neuron was performed over a period of 10–60 min by synchronizing neuronal firing with 1–10 nA positive current delivered in a train of 200-ms on/off intervals (Fig. 3a).

In the four cases of successful double-labeling (U1–U4) shown in Fig. 3b, boutons along retinal afferents were present in apposition to dendrites and/or the cell body of the dura/light-sensitive unit (Fig. 3c; Supplementary Fig. 6). Neuronal responses to light (Fig. 3d) consisted of short-latency (240 ms), short-duration (35 s) and large magnitude (17 spikes/s) in U1; long-latency (6–8 s), long-duration (>100 s) and small magnitude (<5 spike/s) in two units U2, U3; and long-latency (10.5 s), short-duration (13 s) and small magnitude in U4.

Cortical projections of dura/light-sensitive units

The final experiment was aimed at visualizing and mapping the axonal projections of individual thalamic neurons that were identified electrophysiologically as dura/light-sensitive units and filled juxtacellularly with TMR–dextran (Fig. 4a).

In each case, the parent axon projected ipsilaterally through the thalamic reticular nucleus, where it issued a dense collateral terminal field (Fig. 4b), and ascended rostrally through caudate putamen into the external capsule (Fig. 4b,c). The parent axons looped backward within the external capsule, sending branches into multiple cortical regions (Fig. 4d–f). These included the primary somatosensory cortex; primary somatosensory barrel field (S1BF); primary somatosensory trunk region (S1Tr); primary somatosensory dysgranular region (S1DZ); the primary and secondary motor cortices; the retrosplenial agranular cortex (RSA); the parietal association cortex (PtA); the binocular area of the primary visual cortex (V1B); the lateral and mediolateral areas of the secondary visual cortex (V2L, V2ML). Axonal branches within each cortical target extended across layers I through V (Fig. 4d–f).

Discussion

This study revealed a mechanism for the exacerbation of migraine headache by light, whereby neuronal activity of a nociceptive pathway that underlies migraine pain (Supplementary Fig. 7, green) is modulated at the level of the thalamus by retinal photoactivation. We propose that this photomodulation is exerted by novel axonal projections of retinal ganglion cells that converge upon dura-sensitive neurons in a discrete area in the posterior thalamus (Supplementary Fig. 7, red). To a large extent, the retinal projections to the posterior region of the thalamus consisted of axons of ipRGC (Fig. 1; Supplementary Fig. 4), which have been shown to play critical roles in a growing number of non-image-forming functions[17,19–25]. The implication of ipRGC in migraine photophobia

gains support from our finding that exacerbation of migraine headache by light was preserved in blind patients who could sense light in the face of severe degeneration of rod and cone photoreceptors. The mapping of the axonal projections of dura-sensitive thalamic neurons unraveled for the first time the cortical terminal fields of the trigeminovascular pathway.

In migraine patients with normal eyesight, exacerbation of headache by light is likely to involve both extrinsic photoactivation of ipRGC by rods and cones, as well as intrinsic photoactivation of melanopsin[34,35]. The presence of migraine photophobia in blind patients with outer retinal degeneration was associated with the preservation of PLR and circadian photoentrainment, suggesting that non-image-forming pathways remained intact in these patients. Indeed, histological examination of eyes from retinitis pigmentosa patients with total loss of outer photoreceptor layer demonstrated preservation of the melanopsin-expressing ipRGC inner layer[36]. In the case of our photosensitive blind patients, we cannot rule out the possibility that certain aspects of non-visual functions are mediated by functioning rods and cones that survived the retinal disease.

The novel retinal projection to lateral posterior thalamic nuclei and the posterior thalamic nuclear group is distinct from the main visual pathway. This novel projection appeared similar in cases in which a large intravitreal injection of rAAV-GFP produced dense labeling along all known visual pathways and cases in which a small injection produced preferential labeling in the SCN, IGL and OPT – structures that subserve non-image forming functions[22–25]. Since 80% of retinal ganglion cells labeled by the small injection of the tracer expressed melanopsin[22], we conclude that the retinal projections we observed in the posterior thalamus originated to a large extent in ipRGC, and to a lesser extent in non-melanopsinergic RGC.

The photosensitivity of dura-sensitive units in the rat thalamus consisted of short (<1 s) or long (>1 s) response latencies, prolonged discharges, and slow decay of activity. To a limited degree, an instantaneous surge of firing in response to light may be attributed to activation of RGC and ipRGC by rods and cones, whereas subsequent long-lasting activity which subsides slowly in the dark may be attributed to ipRGC signals that are driven intrinsically by melanopsin photoactivation[28,35,37,38]. Photoactivation of dura-sensitive thalamic neurons within hundreds of ms may be consistent with monosynaptic input from retinal ganglion cells triggered by rods and cones. This possibility may be further supported by the close apposition between dura/light-sensitive neurons and boutons of retinal axons in LP and Po observed within 1–1.5-μm-thick scans (Fig. 3c). The number and nature of such close appositions at the level of a distal dendrite, proximal dendrite, or cell body (Fig. 3b) may influence the probability of firing in response to light by individual LP/Po neurons, including response latency, magnitude and duration (Fig. 3d). It should be emphasized, however, that the intrinsic ongoing activity of dura-sensitive thalamic neurons, and the input they continue to receive from the meninges, may mask the onset of their activation by light, and confound the relative contribution of RGC or ipRGC to their response duration and response decay.

The instantaneous induction of neuronal firing in response to light and its slow decay in the dark may be consistent with the exacerbation of migraine headache by light and its slow relief in the dark. Most photosensitive blind migraineurs and those with normal eyesight testify that headache severity increases within few seconds of light exposure and decreases over 10-20 min after return to a dark environment (Supplementary Table 1). Photoactivation of dura-sensitive thalamic units that was delayed by several minutes might be consistent with delayed exacerbation of migraine headache by light reported by some patients (Supplementary Table 1), but cannot be explained at this juncture vis-à-vis the response properties of retinal ganglion cells.

This is the first study to map out the cortical terminal fields of the trigeminovascular pathway. Anterograde transport of tritiated amino acids from the Po to axons in S1 has been traced only to layers I and V[39]. Here we identified singularly-labeled dura-sensitive thalamic neurons that form widespread axonal terminal fields spanning layers I–V of the barrel field and trunk region of the primary somatosensory cortex. While it is generally accepted that the primary somatosensory cortex is involved in certain aspects of the experience of pain[40], the role it plays in processing migraine headache remains to be determined. Additional projections to cortical areas involved in cognitive, motor and visual functions may mediate a number of transient symptoms associated with migraine, such as loss of short-term memory (retrosplenial cortex[41]), muscle weakness and impaired motor coordination (motor cortex[42]), attention deficits (parietal association cortex[43]), and visual disturbances (visual cortex[44],[45]).

Online Methods

Animal and human subjects

Studies were conducted in accordance with NIH guideline and were approved by the institutional committees for human studies and animal care. Twelve blind migraineurs were recruited nationwide through their headache specialists and were interviewed in person. Additional eight were interviewed by phone after responding to national and international announcements disseminated electronically and in print newsletters and magazines serving blind and visually impaired individuals. The interview covered general medical, migraine and visual history; characteristics of migraine attacks and associated symptoms; visual and non-visual photoperception in the presence and absence of migraine. Diagnoses of migraine and visual condition were determined by neuroophthalmologist/headache specialists using information gathered in the interview and available medical charts.

Single-unit recording

Single-unit recording, including surgical preparation and criteria for neuronal responses, were performed as described before[47],[48]. A recording microelectrode was lowered slowly into the posterior thalamus while searching for single-unit responses to repetitive electrical pulses (0.8 ms, 0.5–3.0 mA, 1 Hz) which were applied to the dura through a bipolar electrode at the contralateral transverse sinus. Experiments shown in Fig. 2 were performed under deep urethane anesthesia (1.5 g/kg i.p.) using stainless-steel recording electrodes (1–4 mˆ). Experiments shown in Figs. 3, 4 were performed under isoflurane anesthesia (initially induced with 5%, reduced to 2% during the preparatory surgery, and maintained at 1-1.2%

later on) using glass micropipettes (20 mˆ). Neurons responding to electrical pulses were selected for the study if they also responded to indentation of the dura with calibrated von-Frey monofilament *and* to chemical stimulation of the dura with gelfoam soaked with 1 M KCl. Such dura-sensitive units were tested for photosensitivity by monitoring their ongoing activity in the dark for 10 min before and for 10 min after a 10-s episode of bright light (50,000 lux). Units responding to bright light were also tested with lower light intensities (500 or 3,000 lux). A neuron was classified as photosensitive if its mean rate of firing was 25% greater under 500 lux than in the dark. At the end of each experiment (one neuron/rat), an electrolytic lesion marking the recording site was produced by passing direct anodal current (20 μA for 20 s) through the tip of the electrode. Histological localization of the recording site was determined using microscopic examination of serial coronal sections of the brain.

Co-labeling of retinal afferents and dura/light-sensitive neurons

Retinal afferents were traced anterogradely by injecting 6 μl of 1% CTB into the vitreous body of one eye[22] under brief isoflurane anesthesia. Three days later, dura/light-sensitive neurons were identified using single-unit recording in the contralateral posterior thalamus (one neuron/rat) and filled with 3% TMR–dextran (3,000 MW, anionic, lysine fixable; D-3308, Invitrogen). This was done under deep isoflurane anesthesia, using a procedure of juxtacellular iontophoresis (Fig. 3a) as described elsewhere[49,50]. Four hours later, isoflurane anesthesia was replaced with deep pentobarbital anesthesia (50 mg/kg i.p.), and each rat received transcardiac perfusion with 200 ml heparinized saline, followed by 500 ml of 4% paraformaldehyde, 0.05% picric acid, in 0.1 M phosphate buffered saline (PBS). Brains were removed from the skull, kept in the fixative solution for 2 h, and cryoprotected in 30% sucrose phosphate buffer for 48 h. Brains were then frozen and cut into serial coronal sections (80 μm-thick) using a cryostat (Leica).

For immunolabeling of CTB, free-floating brain sections were pre-incubated for 1 h with 0.1 M PBS containing 0.25% Triton X–100; incubated for 48 h at 4°C with goat primary antibody against CTB (1:50,000 dilution, List Biological Labs); incubated for 2–3 h at room temperature with donkey anti-goat secondary antibody conjugated with Alexa Fluor 488 (1:500 dilution, Invitrogen). Each step was preceded and followed by washes in 0.1 M PBS. Digital imaging was performed using fluorescent light (Leica) or confocal (Zeiss) scanning microscopy that compiled 1–1.5-μm-thick scans using *z*-stacking software. Retinal afferents immunolabeled with Alexa Fluor 488 were detected by excitation at 455 nm and emission at 520 nm (green). Neurons labeled with TMR–dextran were detected in the same set of sections by excitation at 551 nm and emission at 624 nm (red). Co-labeling of the two anterograde tracers was achieved by superimposition of the green and red images (Fig 3b,c; Supplementary Fig. 5).

Mapping of axonal projections of dura/light-sensitive neurons

Dura/light-sensitive thalamic neurons were identified using single-unit recording and filled with TMR–dextran under isoflurane anesthesia as described above. Three days later, rats were perfused with fixative solution, and brains were removed, cryoprotected and cut into sections as described above. Free-floating sections were pretreated for 1 h at room

temperature with 3:1 methanol/PBS solution containing 1% H_2O_2; pre-incubated for 1 h at room temperature in antibody-dilution solution (PBS containing 2% fetal serum albumin, 0.3% Triton X-100); incubated for 48 h at 4°C with rabbit primary antibody against TMR (1:3,000 dilution, Invitrogen); incubated with biotinylated goat anti-rabbit secondary antibody (1:500 dilution, Jackson ImmunoResearch Labs); processed for 2 h with avidin-biotin complex kit (Vector Labs), and detected using nickel-enhanced 3,3′-diaminobenzidine. Each step was preceded and followed by washes in 0.1 M PBS. Immunostained sections were mounted on glass slides, counterstained with thionin and coverslipped. The cell body, dendrites, parent axon and cortical axonal branches of each injected neuron (spanning 20, 36, or 50 consecutive coronal sections/brain) were penciled in aggregate using brightfield microscopy and the camera lucida technique (Fig. 4b,c,e).

Retrograde tracing of afferent projections to the posterior thalamus

Cell bodies of neurons projecting to the posterior thalamic nuclear group were mapped using the retrograde tracer Fluorogold (hydroxystilbamidine, Interchim). A glass micropipette (50 μm tip diameter) loaded with 2% Fluorogold solution was lowered into the dorsal part of the rat posterior thalamic nuclear group under deep isoflurane anesthesia. Iontophoretic release of the tracer was achieved by delivering direct positive current (5–10 μA, on-off cycles, 10 s/cycle) over 10–15 min. After a 4-day recovery period, rats were perfused with fixative solution, and the brain, along with the eyeballs and an upper cervical segment of the spinal cord, were cryoprotected and frozen as described above. Serial coronal sections were collected from the brain and spinal cord (40-μm-thick) and from the eyeballs (25-μm-thick), mounted on glass slides, and coverslipped. The injection site and retrogradely-labeled cell bodies containing Fluorogold were visualized by excitation at 360 nm and emission at 408 nm (blue) using fluorescence microscopy (Leica). Retrogradely-labeled neurons were mapped in the medullary dorsal horn and in C1–C5 using camera lucida tracing (Supplementary Fig. 3). To test whether the retrogradely-labeled retinal ganglion cells included ipRGC units, we repeated the iontophoretic injection of Fluorogold in the posterior thalamic nuclear group described above and processed whole-retina preparations of both eyes for melanopsin immunoreactivity, using rabbit primary antibody against rat melanopsin (1:1,000 dilution, Thermo Scientific) and donkey anti-rabbit secondary antibody conjugated with Alexa Fluor 594 (1:400 dilution, Invitrogen). Immunostained ipRGC units were detected by fluorescence microscopy using excitation at 551 nm and emission at 618 nm (red). Colocalization of melanopsin and Fluorogold was achieved by superimposition of the red and blue images (Supplementary Fig. 4).

Statistical analysis

Rates of neuronal firing were compared between dark and light using Wilcoxon matched-pairs signed-ranks test with a two-tailed level of significance set at $\alpha = 0.05$.

Supplementary Material

Refer to Web version on PubMed Central for supplementary material.

Acknowledgments

This research was supported by NIH grants NS-051484 and NS-035611. Dr. Digre was supported in part by an unrestricted grant from Research to Prevent Blindness, Inc., New York, NY. We thank Drs. Debby Friedman, Ana Recober, Maria Carmen-Wilson and Alexander Mauskop, for sharing their blind migraine patients.

References

1. The International Classification of Headache Disorders, Second Edition. Cephalalgia. 2004; 24:1–160.
2. Selby G, Lance JW. Observations on 500 cases of migraine and allied vascular headache. J Neurol Neurosurg Psychiat. 1960:23–32. [PubMed: 14444681]
3. Markowitz S, Saito K, Moskowitz MA. Neurogenically mediated plasma extravasation in dura mater: effect of ergot alkaloids. A possible mechanism of action in vascular headache. Cephalalgia. 1988; 8:83–91. [PubMed: 3401921]
4. Penfield W, McNaughton F. Dural headache and innervation of the dura mater. Arch, Neurol Psychiat. 1940; 44:43–75.
5. Burstein R, Yamamura H, Malick A, Strassman AM. Chemical stimulation of the intracranial dura induces enhanced responses to facial stimulation in brain stem trigeminal neurons. Journal of Neurophysiology. 1998; 79:964–982. [PubMed: 9463456]
6. Strassman AM, Raymond SA, Burstein R. Sensitization of meningeal sensory neurons and the origin of headaches. Nature. 1996; 384:560–564. [PubMed: 8955268]
7. Burstein R, Yarnitsky D, Goor-Aryeh I, Ransil BJ, Bajwa ZH. An association between migraine and cutaneous allodynia. Annals Neurol. 2000; 47:614–624.
8. Burstein R, Cutrer FM, Yarnitsky D. The development of cutaneous allodynia during a migraine attack: clinical evidence for the sequential recruitment of spinal and supraspinal nociceptive neurons in migraine. Brain. 2000; 123:1703–1709. [PubMed: 10908199]
9. Kawasaki A, Purvin VA. Photophobia as the presenting visual symptom of chiasmal compression. J Neuroophthalmol. 2002; 22:3–8. [PubMed: 11937897]
10. Liveing, E. On megrim, sick headache. Arts & Boeve Publishers; Nijmegen: 1873.
11. Lebensohn JE. Photophobia: mechanism and implications. American journal of ophthalmology. 1951; 34:1294–1300. [PubMed: 14877953]
12. Aurora SK, Cao Y, Bowyer SM, Welch KM. The occipital cortex is hyperexcitable in migraine: experimental evidence. Headache. 1999; 39:469–476. [PubMed: 11279929]
13. Lamonte M, Silberstein SD, Marcelis JF. Headache associated with aseptic meningitis. Headache. 1995; 35:520–526. [PubMed: 8530275]
14. Welty TE, Horner TG. Pathophysiology and treatment of subarachnoid hemorrhage. Clin Pharm. 1990; 9:35–39. [PubMed: 2406101]
15. Lowenfeld, I. The dazzling syndrome. Wane State University Press; Detroit: 1993.
16. Miller, NR. Photophobia. In: Miller, NR., editor. Walsh and Hoyt's clinical neuro-ophthlmology. Williams&Wilkins; Baltimore: 1985. p. 1099-1106.
17. Lucas RJ, Douglas RH, Foster RG. Characterization of an ocular photopigment capable of driving pupillary constriction in mice. Nat Neurosci. 2001; 4:621–626. [PubMed: 11369943]
18. Klein DC, Weller JL. Rapid light-induced decrease in pineal serotonin N-acetyltransferase activity. Science (New York, NY. 1972; 177:532–533.
19. Freedman MS, et al. Regulation of mammalian circadian behavior by non-rod, non-cone, ocular photoreceptors. Science (New York, NY. 1999; 284:502–504.
20. Hattar S, et al. Melanopsin and rod-cone photoreceptive systems account for all major accessory visual functions in mice. Nature. 2003; 424:76–81. [PubMed: 12808468]
21. Lucas RJ, Freedman MS, Munoz M, Garcia-Fernandez JM, Foster RG. Regulation of the mammalian pineal by non-rod, non-cone, ocular photoreceptors. Science (New York, NY. 1999; 284:505–507.

22. Gooley JJ, Lu J, Fischer D, Saper CB. A broad role for melanopsin in nonvisual photoreception. J Neurosci. 2003; 23:7093–7106. [PubMed: 12904470]
23. Guler AD, et al. Melanopsin cells are the principal conduits for rod-cone input to non-image-forming vision. Nature. 2008; 453:102–105. [PubMed: 18432195]
24. Hattar S, et al. Central projections of melanopsin-expressing retinal ganglion cells in the mouse. The Journal of comparative neurology. 2006; 497:326–349. [PubMed: 16736474]
25. Hannibal J, Fahrenkrug J. Target areas innervated by PACAP-immunoreactive retinal ganglion cells. Cell Tissue Res. 2004; 316:99–113. [PubMed: 14991397]
26. Provencio I, Jiang G, De Grip WJ, Hayes WP, Rollag MD. Melanopsin: An opsin in melanophores, brain, and eye. Proc Natl Acad Sci U S A. 1998; 95:340–345. [PubMed: 9419377]
27. Provencio I, et al. A novel human opsin in the inner retina. J Neurosci. 2000; 20:600–605. [PubMed: 10632589]
28. Berson DM, Dunn FA, Takao M. Phototransduction by retinal ganglion cells that set the circadian clock. Science (New York, NY. 2002; 295:1070–1073.
29. Hattar S, Liao HW, Takao M, Berson DM, Yau KW. Melanopsin-containing retinal ganglion cells: architecture, projections, and intrinsic photosensitivity. Science (New York, NY. 2002; 295:1065–1070.
30. Panda S, et al. Melanopsin is required for non-image-forming photic responses in blind mice. Science (New York, NY. 2003; 301:525–527.
31. Malick A, Jakubowski M, Elmquist JK, Saper CB, Burstein R. A neurohistochemical blueprint for pain-induced loss of appetite. Proc Natl Acad Sci U S A. 2001; 98:9930–9935. [PubMed: 11504950]
32. Zagami AS, Lambert GA. Stimulation of cranial vessels excites nociceptive neurones in several thalamic nuclei of the cat. Experimental Brain Research. 1990; 81:552–566. [PubMed: 2226688]
33. Davis KD, Dostrovsky JO. Properties of feline thalamic neurons activated by stimulation of the middle meningeal artery and sagittal sinus. Brain research. 1988; 454:89–100. [PubMed: 3409027]
34. Dacey DM, et al. Melanopsin-expressing ganglion cells in primate retina signal colour and irradiance and project to the LGN. Nature. 2005; 433:749–754. [PubMed: 15716953]
35. Wong KY, Dunn FA, Graham DM, Berson DM. Synaptic influences on rat ganglion-cell photoreceptors. The Journal of physiology. 2007; 582:279–296. [PubMed: 17510182]
36. Hannibal J, et al. Melanopsin is expressed in PACAP-containing retinal ganglion cells of the human retinohypothalamic tract. Investigative ophthalmology & visual science. 2004; 45:4202–4209. [PubMed: 15505076]
37. Berson DM. Phototransduction in ganglion-cell photoreceptors. Pflugers Arch. 2007; 454:849–855. [PubMed: 17351786]
38. Tu DC, et al. Physiologic diversity and development of intrinsically photosensitive retinal ganglion cells. Neuron. 2005; 48:987–999. [PubMed: 16364902]
39. Herkenham M. Laminar organization of thalamic projections to the rat neocortex. Science (New York, NY. 1980; 207:532–535.
40. Ingvar, M.; Hsieh, JC. The image of pain. In: Wall, PD.; Melzack, R., editors. Textbook of Pain. Churchill Livingston; London: 1999. p. 215-233.
41. Valenstein E, et al. Retrosplenial amnesia. Brain. 1987; 110(Pt 6):1631–1646. [PubMed: 3427404]
42. Donchin O, Gribova A, Steinberg O, Bergman H, Vaadia E. Primary motor cortex is involved in bimanual coordination. Nature. 1998; 395:274–278. [PubMed: 9751054]
43. Mountcastle VB, Lynch JC, Georgopoulos A, Sakata H, Acuna C. Posterior parietal association cortex of the monkey: command functions for operations within extrapersonal space. J Neurophysiol. 1975; 38:871–908. [PubMed: 808592]
44. Lowel S, Singer W. Selection of intrinsic horizontal connections in the visual cortex by correlated neuronal activity. Science (New York, NY. 1992; 255:209–212.
45. Livingstone MS, Hubel DH. Anatomy and physiology of a color system in the primate visual cortex. J Neurosci. 1984; 4:309–356. [PubMed: 6198495]
46. Paxinos, G.; Watson, C. The Rat Brain in Stereotaxic Coordinates. Academic Press; Orlando: 1998.

47. Burstein R, Jakubowski M. Analgesic triptan action in an animal model of intracranial pain: A race against the development of central sensitization. Ann Neurol. 2004; 55:27–36. [PubMed: 14705109]

48. Yamamura H, Malick A, Chamberlin NL, Burstein R. Cardiovascular and neuronal responses to head stimulation reflect central sensitization and cutaneous allodynia in a rat model of migraine. Journal of Neurophysiology. 1999; 81:479–493. [PubMed: 10036252]

49. Pinault D. A novel single-cell staining procedure performed in vivo under electrophysiological control: Morpho-functional features of juxtacellularly labeled thalamic cells and other central neurons with biocytin or Neurobiotin. Journal of Neuroscience Methods. 1996; 65:113–136. [PubMed: 8740589]

50. Gauriau C, Bernard JF. Posterior triangular thalamic neurons convey nociceptive messages to the secondary somatosensory and insular cortices in the rat. J Neurosci. 2004; 24:752–761. [PubMed: 14736861]

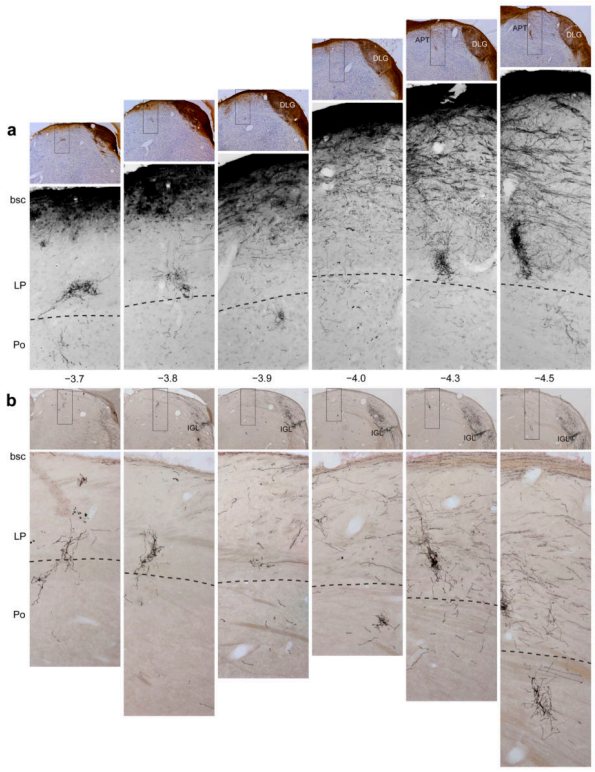

Figure 1.

Projections of retinal ganglion cells to the lateral posterior thalamic nuclei (LP) and posterior thalamic nuclear group (Po). Retrograde tracing of retinal afferents was performed using large (**a**) or small (**b**) injections of rAAV–GFP into the vitreous body of the eye (see text for details). (**a**) Top panels: low-power images of coronal sections counterstained with thionin, showing immunolabeled retinal afferents (brown) in the main visual pathway. Bottom panels: high-power detail of the boxed areas in the corresponding top panels, showing retinal afferents in ventral LP and dorsal Po. These images display only the blue channel which isolated the labeled fibers from the background Nissl staining. (**b**) Top panels: low-power images of coronal sections showing preferential labeling of retinal afferents in the intergeniculate leaflet (IGL). Bottom panels: high-power detail of the boxed areas in the corresponding top panels, showing immunolabeled retinal afferents in ventral LP and dorsal Po. Preferential labeling of non-image-forming pathways by the smaller rAAV–GFP injection (**b**) compared with the larger injection (**a**) reflects preferential labeling of ipRGC (see text for explanation). Note that the retinal afferents run dorsoventrally from the main visual pathway through ventral aspect of LP and into dorsal aspect of Po (**a,b**). Note that the density of labeled axons in ventral LP and dorsal Po is similar between **a** and **b,** suggesting that most labeled axons in these areas were of ipRGC origin. Numbers indicate distance from Bregma (mm). Abbreviations: APT, anterior pretectal nucleus; bsc, brachium superior colliculus; DLG, dorsal part of lateral geniculate nucleus. Scale bars represent 500 μm.

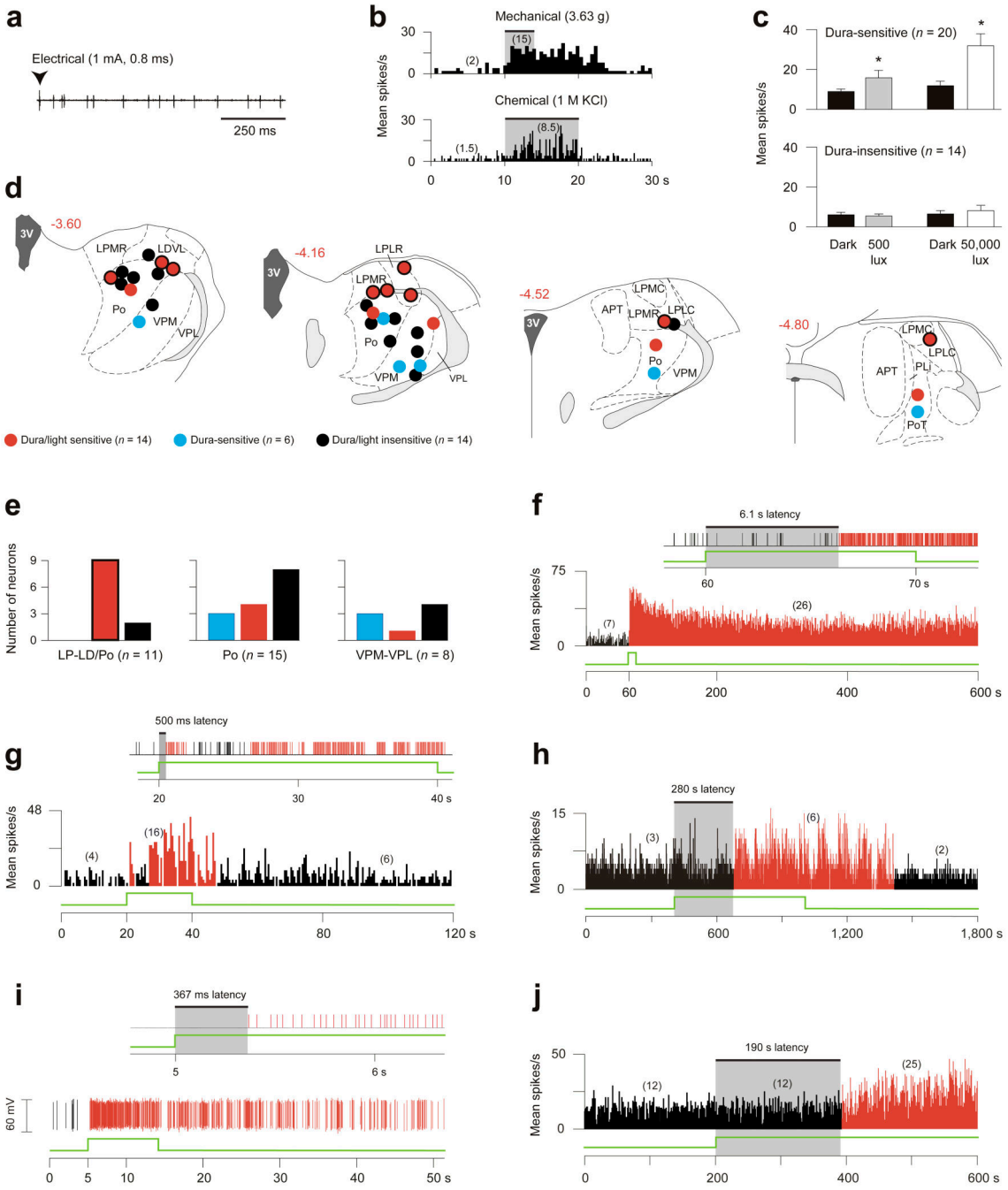

Figure 2.

Photosensitivity of dura-sensitive thalamic neurons. (**a,b**) Identifying neuronal responses to electrical (**a**), mechanical and chemical (**b**) stimulation of the dura. (**c**) Effects of ambient light (500 lux) and bright light (50,000 lux) on firing rate (mean ± s.e.m.) of dura-sensitive *vs.* dura-insensitive thalamic neurons (*$P < 0.05$; Wilcoxon matched-pairs signed-ranks test). (**d**) Histological localization of the recorded neurons. Drawings and numbers indicating distance from Bregma (mm) are based on Paxinos and Watson[46]. For abbreviations see text. (**e**) Graphic representation of the dorso-ventral localization of the

neurons shown in **d**. Color coding same as in **d**; bordered red bar in left panel corresponds to bordered red circles in **d**. (**f–j**) Examples of delayed and immediate photoactivation of individual dura-sensitive thalamic neurons by 50,000 (**f,g**), 3,000 (**h,i**) and 500 lux (**j**) of white light (green line). Panels **f, g** consist of window discriminator spike output (top) and mean activity histogram (bottom). Panels **h, j** show mean activity histogram. Panel **i** consists of window discriminator output (top) and oscillographic tracing (bottom). Each of the light intensities induced delayed activation in some neurons (**f,h,j**) and immediate activation in others (**g,i**). Each of the light intensities induced prolonged activation that outlasted the stimulus by several minutes. Numbers in parentheses indicate mean spikes/s for the corresponding interval. Black and red bars indicate, respectively, baseline and enhanced periods of activity in response to light. Bin width are 0.5 (**f,g,j**) and 1 s (**h**).

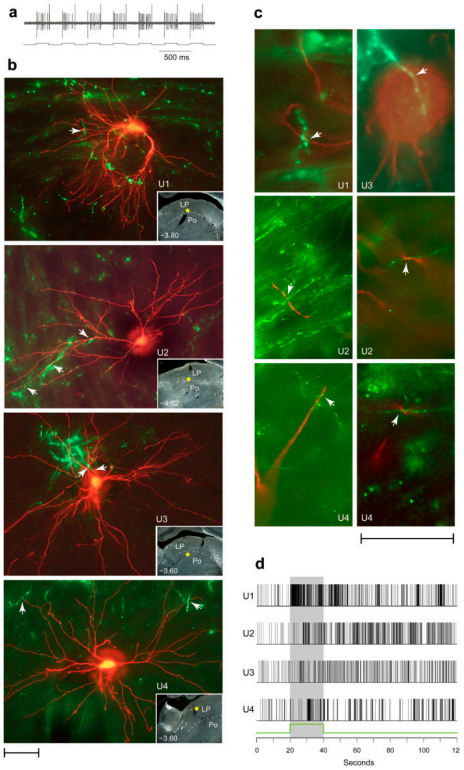

Figure 3.

Close apposition between dura/light-sensitive neurons and retinal afferents in LP and Po. (**a**) Synchronization of neuronal activity (top trace) with the current (bottom trace) delivered by the TMR–dextran filled recording micropipette (see text for detail). (**b**) Dura/light sensitive units (U1–U4) filled with TMR–dextran (red) and retinal axons labeled anterogradely with CTB (green). Each image represents z-stacking of approximately thirty 1–1.5-μm-thick scans. Arrowheads point to potential axodendritic or axosomatic apposition. Localization of each cell body is marked by a yellow star in the low-power, darkfield inset. Numbers indicate distance from Bregma. (**c**) Evidence for axodendritic and axosomatic apposition within a single 1–1.5-μm-thick scan taken from the units shown in **b**. (**d**) Neuronal firing in response to 50,000 lux of white light (green line and shaded area), corresponding to the individual neurons shown in **b**. Scale bars represent 50 μm (**b,c**).

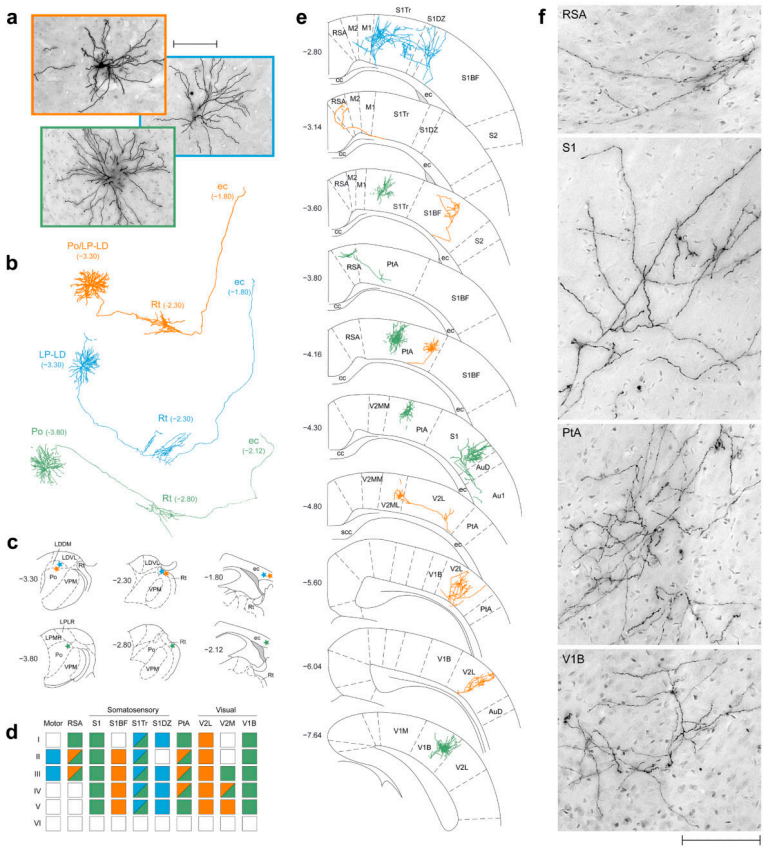

Figure 4.

Cortical projections of three dura/light-sensitive thalamic neurons juxtacellularly-filled with TMR–dextran. (**a**) Labeled cell bodies and their dendrites in the posterior thalamus. (**b**) Camera-lucida tracing of the cell bodies, dendrites, and axonal trajectories coursing through thalamic reticular nucleus (Rt) en route the external capsule (ec). (**c**) Localization of cell bodies, Rt collaterals and entry point of the parent axon into the external capsule. (**d**) Tabulation of cortical areas and layers containing axons with synaptic boutons. (**e**) Camera-lucida tracing of axon terminal fields in different cortical areas. (**f**) Photomicrographs of axons with synaptic boutons in several cortical areas. Drawings and numbers (**b,c,e**) indicating distance from Bregma (mm) are based on Paxinos and Watson[46]. Au1, primary auditory cortex; AuD, secondary auditory cortex, dorsal; M1 and M2, primary and secondary motor cortices, respectively; S1, primary somatosensory cortex. For other abbreviations not listed here see text. Scale bars represent 100 μm (**a**,**f**).

Table 1

Incidence of photosensitivity during migraine in blind persons

				Manifestation of photosensitivity					
Diagnosis	**Eyeballs**	**PLR**	**Sleep cycle**	**Migraine-free**	**During migraine**	**Migraine with aura**	**Age**	**Age at first attack**	**Migraine d/mon**
Without light perception (*n* = 6)									
Retinal prematurity	Enucleated	–	Irregular	None	None	No	51	7	1
Retinal prematurity, secondary glaucoma	Enucleated	–	Fragmented	None	None	No	56	22	8
Retinal cancer	Enucleated	–	Fragmented	None	None	No	34	32	3
Congenital syphilis, secondary glaucoma	Enucleated	–	Fragmented	None	None	No	55	13	1
Bilateral optic neuropathy	Present	No	Fragmented	None	None	Yes	41	37	2
Posterior ischemic optic neuropathy	Present	n/a	Fragmented	None	None	Yes	71	18	4
With light perception (*n* = 14)									
Retinitis pigmentosa	present	Yes	Regular	None	Headache ↑	No	57	3	0.5
Retinitis pigmentosa	present	Yes	Fragmented	Unpleasant	Headache ↑	Yes	41	12	12
Leber's congenital amaurosis	present	Yes	Regular	Unpleasant	Headache ↑	Yes	43	22	6
Leber's congenital amaurosis	present	Yes	Regular	None	Headache ↑	No	21	3	5
Cones/rods dystrophy	present	Yes	Regular	Unpleasant	Headache ↑	No	39	7	2
Cones/rods dystrophy	present	Yes	Regular	None	Headache ↑	No	17	12	2
Cones/rods dystrophy	present	Yes	Regular	None	Headache ↑	No	19	6	8
Retinal degeneration	present	n/a	Fragmented	Unpleasant	Headache ↑	Yes	55	30	4
Retinal prematurity	present	n/a	Regular	Ocular pain	Headache ↑	No	28	25	1
Retinal prematurity	present	Yes	Fragmented	None	Headache ↑	No	55	8	1
Retinal prematurity	present	Yes	Regular	None	Headache ↑	Yes	29	8	30
Bilateral optic neuropathy	Present	Yes	Regular	None	Headache ↑	No	60	50	4
Bilateral retinal detachment and glaucoma	Present	Yes	Regular	Ocular pain	Headache ↑	Yes	45	7	4
Posterior ischemic optic neuropathy	Present	Yes	Regular	None	Headache ↑	No	54	33	30

n/a, not available